

Diffusion kurtosis imaging and diffusion-weighted imaging-based classification of acute stroke lesions in the brain: A pilot study

Xin Liu

Xiamen Medical College Affiliated Second Hospital

Songsen Chen

Xiamen Medical College Affiliated Second Hospital

Fang Chen

Xiamen Medical College Affiliated Second Hospital

Lei Wang

Xiamen Medical College Affiliated Second Hospital

Khan Afsar

Electronic science and technology Xiamen University

Gang Guo

Xiamen Medical College Affiliated Second Hospital

Gen Yan (✉ gyan@stu.edu.cn)

Xiamen Medical College Affiliated Second Hospital

Research article

Keywords: diffusion kurtosis imaging, acute stroke, classification, prognosis, diffusion-weighted imaging

Posted Date: May 27th, 2020

DOI: <https://doi.org/10.21203/rs.3.rs-27738/v1>

License:   This work is licensed under a Creative Commons Attribution 4.0 International License.

[Read Full License](#)

Abstract

Background: We postulated that diffusion kurtosis imaging (DKI) could classify heterogeneous stroke lesions on diffusion-weighted imaging (DWI) and improve our understanding of the characteristics of tissue injury. We aimed to retrospectively study different DKI parameters in patients with acute stroke reported in the literature.

Methods: We collected the DWI and DKI data of 41 patients (26 men, 15 women), including 86 cases of acute cerebral infarction in different brain regions. Of them, 20 patients had single infarction, whereas others had multiple infarctions. Acute cerebral infarction lesions were classified into two categories based on DKI and DWI parameters: type I, matched DKI and DWI parameters and type II, mismatched DKI and DWI parameters. Regions of interest (ROIs) were outlined within the most severely infarcted areas of each lesion according to each independent parametric map. In the control groups, same-sized ROIs were located in the corresponding region of the normal contralateral hemisphere. In both categories, DKI and DWI parameters followed a normal Gaussian distribution. We used the independent sample t-test to compare the differences in each group.

Results: In type I cases, fractional anisotropy, mean diffusivity, axial diffusivity, radial diffusivity, mean kurtosis (MK), and axial kurtosis (Ka) values were significantly different ($P < 0.05$). In type II cases, only MK and Ka values were significantly different ($P < 0.05$).

Conclusions: DKI can provide more information on acute ischemic brain infarction and enrich our understanding of ischemic tissue injury. This DKI and DWI parameters-based classification of acute stroke lesions may confer a renewed understanding of infarction cores.

Background

Diffusion-weighted magnetic resonance imaging (DWI) has become an integral part of the clinical evaluation of acute stroke because of its high detection sensitivity for cerebral infarctions¹. Although medical imaging and treatment have advanced, current research is not limited to the detection of ischemic lesions and aimed at distinguishing reversible and irreversible brain damage.

Previous studies suggest that the mismatch between DWI and perfusion-weighted imaging showed marked sensitivity to ischemic brain injury (Fig. 1)^{1,2}. Nevertheless, the significance of tissue mismatch, including those of oligemic, salvageable, and irretrievable tissue, is unclear. These tissue characteristics may depend on various intricate factors, such as the duration and nature of the ischemic injury, proximity of the patent vessels, and so on. In conclusion, perfusion-diffusion mismatch can only approximate the features of real ischemic penumbra. Despite the limitations, this mismatch often guides clinical decisions in the management of acute stroke³. Therefore, presently, additional methods are being explored to provide a profound knowledge of ischemic brain injury.

Diffusion kurtosis imaging (DKI) is a promising new DWI sequence that measures the non-Gaussianity of water diffusion and can be used to characterize the complexity or heterogeneity of tissue microenvironments with reduced imaging time, hardware requirements, and post-processing effort compared with 3-dimensional q-space imaging⁴. Indeed, DKI has been reported to detect microstructural cerebral changes in aging brains, acute stroke, and tumors.

We postulated that DKI could stratify heterogeneous DWI lesions and improve the characterization of tissue injury. The spatiotemporal dynamics of DKI in patients with acute stroke have been studied systematically in the literature.

Methods

Ethics Statement

The study was approved by the institutional review board of the Second Affiliated Hospital of Xiamen Medical University. The patients (conscious patients) or their lineal relatives (for the unconscious patients) provided written informed consent. The study adhered to the tenets of the Declaration of Helsinki.

Subjects

Overall, 41 patients (26 men, 15 women) with 86 different cases of acute cerebral infarction in different areas of the brain were recruited for this study. Twenty patients had single infarction, whereas the others had multiple infarctions. All patients underwent MRI scans within 72 h of stroke onset. The inclusion criterion was presence of acute cerebral infarction. The exclusion criteria were presence of cerebral hemorrhage (original or secondary), cerebral tumors, degenerative brain disease, craniocerebral trauma, post-craniocerebral operation, dyspnea, and coma.

Classification

Herein, we classified acute cerebral infarction lesions into two categories according to the manifestations of DKI and DWI parameters. Type I lesions had matched DKI and DWI parameters, and type II lesions had mismatched DKI and DWI parameters. This study included 45 and 41 cases of type I and type II lesions, respectively (Fig. 2–3).

Imaging acquisition

All images were acquired using a GE 1.5-Tesla HDx Echo Speed Plus MRI scanner with an 8-channel head coil (GE Healthcare Life Sciences, Chalfont, UK). The scanning sequences included T1-weighted imaging (T1WI), T2-weighted imaging (T2WI), T2-weighted fluid-attenuated inversion recovery (T2-FLAIR) imaging, DWI, and DKI. The b-value of the DWI sequence was 1000s/mm². The DKI sequence parameters were as follows: repetition time (TR), 6000 ms; echo time (TE), minimum; layer thickness, 5 mm; layer spacing,

1.5 mm; field of view (FOV), 240 × 240 mm²; matrix, 96 × 130; layer number, 19; diffusion direction, 15; b = 0, 1000, and 2000s/mm²; and scanning time, approximately 6 m and 18 s.

Imaging analysis

DKI post-processing software provided by GE was used for the post-processing of DKI images. Regions of interest (ROIs; maximal area in the center of the lesion) were outlined within the most severely infarcted areas of each lesion according to each independent parametric map. In the control groups, same-sized ROIs were located in the corresponding normal regions of the contralateral hemisphere (Fig. 4). Multiple DKI parameters [mean kurtosis (MK), radial kurtosis (Kr), and axial kurtosis (Ka)] were measured for all ROIs. Two radiologists independently diagnosed and analyzed the ischemic lesions. In case of disagreements, a third radiologist was consulted.

Statistical analysis

The relative diagnostic value of DKI parameters was analyzed with the independent sample t-test. Statistical analyses were performed using SPSS 13.0 software (SPSS, Inc., Chicago, IL, USA). P-values < 0.05 were considered statistically significant.

Results

Patient characteristics

This study included 41 patients with acute ischemic stroke, including 26 men and 15 women aged 63.4 ± 15.6 years (range, 30–83 years). Overall, 86 groups of ROIs were outlined in different regions of the brain in patients with stroke lesions, whereas the same number of ROIs were outlined in the contralateral areas of normal brains in the control group.

Parametric maps of DKI in different types of stroke lesions

All DKI and DWI parameters had normal distribution in both type I and type II lesions. An independent sample t-test was used to compare the differences between the parameters in each group. Parametric maps of DKI for acute stroke lesions are presented in Figs. 5 and 6. Values of fractional anisotropy (FA), mean diffusivity (MD), axial diffusivity (Da), and radial diffusivity (Dr) were less compared with those of the contralateral normal group, whereas the values of MK, Ka, and Kr were remarkably high.

In type I lesions, values of FA, MD, Da, Dr, MK, and Ka were statistically different (P < 0.05), while in type II, only the MK and Ka values were statistically different (P < 0.05; Table 1).

Table 1

	Type I			Type II		
	Ischemia	Contralateral	P value	Ischemia	Contralateral	P value
FA	0.23	0.42	0.000	0.32	0.44	0.001
MD	0.66	1.02	0.000	0.96	0.97	0.944
Da	0.82	1.5	0.000	1.24	1.51	0.084
Dr	0.58	0.78	0.000	0.82	0.74	0.528
MK	1.22	0.86	0.000	1.12	0.89	0.000
Ka	1.34	0.81	0.000	1.17	0.79	0.000
Kr	1.15	0.93	0.054	1.08	0.98	0.341

Discussion

DWI is the most reliable neuroimaging technique for the assessment of acute ischemic stroke⁵. DWI has been used extensively in the clinical diagnosis of acute stroke because of its high sensitivity. However, DWI cannot reflect the real tissue damage in acute stroke lesions, which are heterogeneous, or show the partial recovery during treatment⁶. The ischemic core appears hyperintense on DWI with an obvious reduction in the apparent diffusion coefficient (ADC). Generally, ADC values remain low for up to 4 days after a stroke; thereafter, it demonstrates gradual pseudonormalization. In the subacute or chronic stage of stroke, ADC values normalize or remain high⁷. A fundamental limitation of ADC is that it can only be used to analyze the approximate date of stroke formation by assessing the Gaussian distribution; however, cerebral infarction lesions have a non-Gaussian distribution.

Coefficient of DK (K) represents the quantitative measurement of the non-Gaussianity of the diffusion in both the white matter (WM) and gray matter (GM). In biological tissues, water diffusion is restricted owing to multiple barriers, such as the cellular/axonal membranes, organelles, and/or compartments, resulting in positive K values⁸. High K values of ischemic lesions may indicate an increase in the complexity of the aqueous microenvironment or heterogeneity in the WM and GM.

A previous study showed that in an experimental model of traumatic brain injury, the MK elevates in neural tissues subjected to subacute stage infarction despite pseudonormalization of MD and FA values⁹. An increase in the MK was associated with increased reactive astrogliosis, which confirms that K is a biomarker of tissue heterogeneity. Similar results were also observed in previous preliminary studies of animals and humans with stroke using DKI.

In other words, K is an in vivo measurement of the complications or/and inhomogeneity of the microenvironment of stroke lesions. It provides complementary information to conventional diffusion indices and maybe a more sensitive biomarker to assess the pathophysiological changes associated with stroke¹⁰.

The results of our study imply that DWI/DKI mismatch may be indicative of a mildly damaged and potentially recoverable ischemic lesion, whereas the matched areas may be indicative of irreparable

cellular damage. Here, the type II stroke lesions showed significantly different MK and Ka values, which may be an indicative mismatch of the real infarction core in patients with acute stroke.

Conclusions

DKI can provide more information than DWI about acute ischemic infarction lesions of the brain and facilitate improved understanding of ischemic tissue injuries. Our method of classification of acute stroke lesions based on their DKI and DWI parameters may enable further understanding of the real infarction core.

List Of Abbreviations

diffusion kurtosis imaging (DKI)

diffusion-weighted imaging (DWI)

mean kurtosis (MK)

axial kurtosis (Ka)

radial kurtosis (Kr)

T1-weighted imaging (T1WI)

T2-weighted imaging (T2WI)

T2-weighted fluid-attenuated inversion recovery (T2-FLAIR)

repetition time (TR)

echo time (TE)

Values of fractional anisotropy (FA)

mean diffusivity (MD)

axial diffusivity (Da)

radial diffusivity (Dr)

apparent diffusion coefficient (ADC)

Declarations

Ethics approval and consent to participate

The study was approved by the institutional review board of the Second Affiliated Hospital of Xiamen Medical University. The patients (conscious patients) or their lineal relatives (for the unconscious patients) provided written informed consent. The study adhered to the tenets of the Declaration of Helsinki.

Consent for publication

Not Applicable.

Availability of data and materials

The datasets used and/or analyzed during the current study are available from the corresponding author on reasonable request.

Competing interests

The authors declared that they have no conflicts of interest related to this work. We declare that we do not have any commercial or associated interests that represent a conflict of interest in connection with the work submitted.

Funding

Supported by Science and Technology Program of Fujian Province of China (No. 2017D017); The Joint Funds for the Health and Education of Fujian Province, China (No. 2019-WJ-31), Institute of Respiratory Diseases, Xiamen Medical College (No. HXJB-15)

Authors' contributions

X.L., G.G., and G.Y. conceived and designed the experiments. X.L., F.C., L.W., and K.A. performed the experiments and collected the data. X.L. and Ss C drafted the paper. All authors read and approved the final manuscript.

Acknowledgements

Not applicable.

Authors' information

Xin Liu¹, Songsen Chen¹, Fang Chen¹, Lei Wang¹, Khanafsar², Gang Guo¹, and Gen Yan¹

¹Department of Radiology, The Second Affiliated Hospital of Xiamen Medical College, Xiamen, Fujian Province 361023, China

²Electronic science and technology Xiamen university, Xiamen, Fujian Province 361023, China

Fist Author

Xin Liu, youranxin@yeah.net

Corresponding Author

Gen Yan, gyan@stu.edu.cn

References

1. Wittsack HJ, Ritzl A, Fink GR, Wenserski F, Siebler M, Seitz RJ, et al. MR imaging in acute stroke: diffusion-weighted and perfusion imaging parameters for predicting infarct size. *Radiology*. 2002;222:397-403.
2. Yin J, Sun H, Wang Z, Ni H, Shen W, Sun PZ. Diffusion kurtosis imaging of acute infarction: comparison with routine diffusion and follow-up MR imaging. *Radiology*. 2018;287:651-7.
3. Chen Y, Zhao X, Ni H, Feng J, Ding H, Qi H, et al. Parametric mapping of brain tissues from diffusion kurtosis tensor. *Comput Math Methods Med*. 2012;2012:820847.
4. Jensen JH, Falangola MF, Hu C, Tabesh A, Rapalino O, Lo C, et al. Preliminary observations of increased diffusional kurtosis in human brain following recent cerebral infarction. *NMR Biomed*. 2011;24:452-7.
5. Zhu LH, Zhang ZP, Wang FN, Cheng QH, Guo G. Diffusion kurtosis imaging of microstructural changes in brain tissue affected by acute ischemic stroke in different locations. *Neural Regen Res*. 2019;14:272-9.
6. Hui ES, Fieremans E, Jensen JH, Tabesh A, Feng W, Bonilha L, et al. Stroke assessment with diffusional kurtosis imaging. *Stroke*. 2012;43:2968-73.
7. Guo YL, Li SJ, Zhang ZP, Shen ZW, Zhang GS, Yan G, et al. Parameters of diffusional kurtosis imaging for the diagnosis of acute cerebral infarction in different brain regions. *Exp Ther Med*. 2016;12:933-8.
8. Zhou IY, Guo Y, Igarashi T, Wang Y, Mandeville E, Chan ST, et al. Fast diffusion kurtosis imaging (DKI) with Inherent COrrrelation-based Normalization (ICON) enhances automatic segmentation of heterogeneous diffusion MRI lesion in acute stroke. *NMR Biomed*. 2016;29:1670-7.
9. Steven AJ, Zhuo J, Melhem ER. Diffusion kurtosis imaging: an emerging technique for evaluating the microstructural environment of the brain. *AJR Am J Roentgenol*. 2014;202:26-33.
10. Weber RA, Hui ES, Jensen JH, Nie X, Falangola MF, Helpert JA, et al. Diffusional kurtosis and diffusion tensor imaging reveal different time-sensitive stroke-induced microstructural changes. *Stroke*. 2015;46:545-50.
11. Zhang S, Yao Y, Shi J, Tang X, Zhao L, Zhu W. The temporal evolution of diffusional kurtosis imaging in an experimental middle cerebral artery occlusion (MCAO) model. *Magn Reson Imaging*. 2016;34:889-95.

12. Hui ES, Du F, Huang S, Shen Q, Duong TQ. Spatiotemporal dynamics of diffusional kurtosis, mean diffusivity and perfusion changes in experimental stroke. *Brain Res.* 2012;1451:100-9.
13. Leslie-Mazwi TM, Hirsch JA, Falcone GJ, Schaefer PW, Lev MH, Rabinov JD, et al. Endovascular stroke treatment outcomes after patient selection based on magnetic resonance imaging and clinical criteria. *JAMA Neurol.* 2016;73:43-9.
14. Jensen JH, Falangola MF, Hu C, Tabesh A, Rapalino O, Lo C, et al. Preliminary observations of increased diffusional kurtosis in human brain following recent cerebral infarction. *NMR Biomed.* 2011;24:452-7.
15. Cheung JS, Wang E, Lo EH, Sun PZ. Stratification of heterogeneous diffusion MRI ischemic lesion with kurtosis imaging: evaluation of mean diffusion and kurtosis MRI mismatch in an animal model of transient focal ischemia. *Stroke.* 2012;43:2252-4.
16. Weber RA, Hui ES, Jensen JH, Nie X, Falangola MF, Helpert JA, et al. Diffusional kurtosis and diffusion tensor imaging reveal different time-sensitive stroke-induced microstructural changes. *Stroke.* 2015;46, 545-50.
17. Inoue M, Mlynash M, Christensen S, Wheeler HM, Straka M, Tipirneni A, et al. Early diffusion-weighted imaging reversal after endovascular reperfusion is typically transient in patients imaged 3 to 6 hours after onset. *Stroke.* 2014;45:1024-8.
18. Guo Y, Zhou IY, Chan ST, Wang Y, Mandeville ET, Igarashi T, et al. pH-sensitive MRI demarcates graded tissue acidification during acute stroke - pH specificity enhancement with magnetization transfer and relaxation-normalised amide proton transfer (APT) MRI. *Neuroimage.* 2016;141:242-9.

Figures

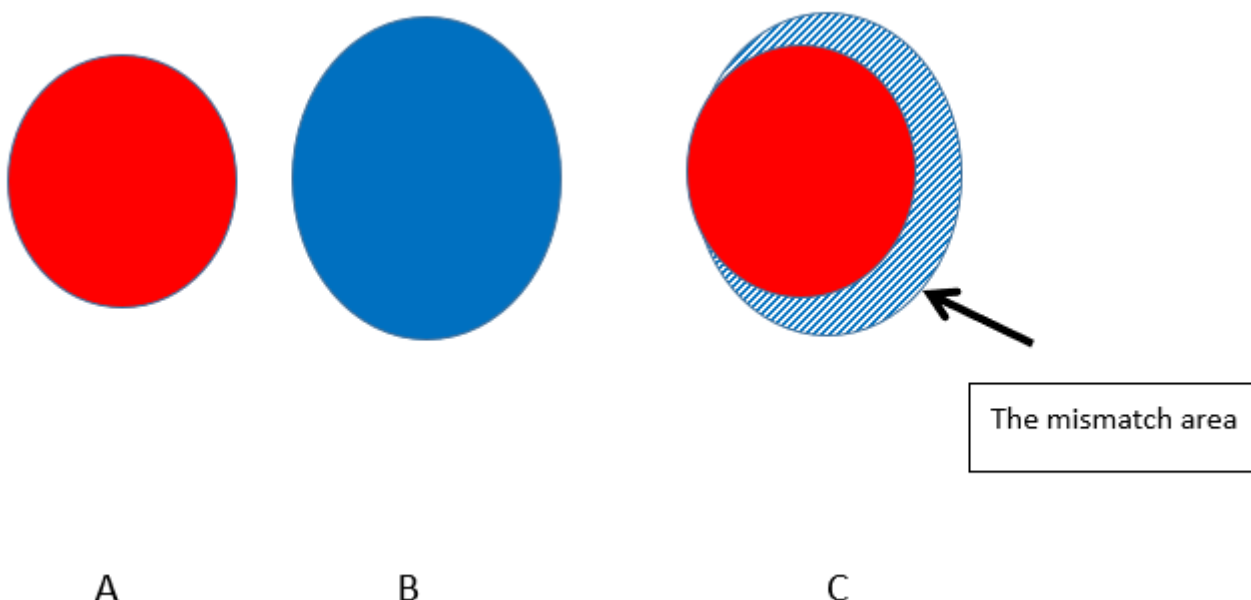


Figure 1

The red circle (A) indicates the stroke lesion seen on the DWI scan, while the blue circle (B) indicates the stroke lesion seen on the PWI scan; C indicates the mis-match of the DWI and PWI.

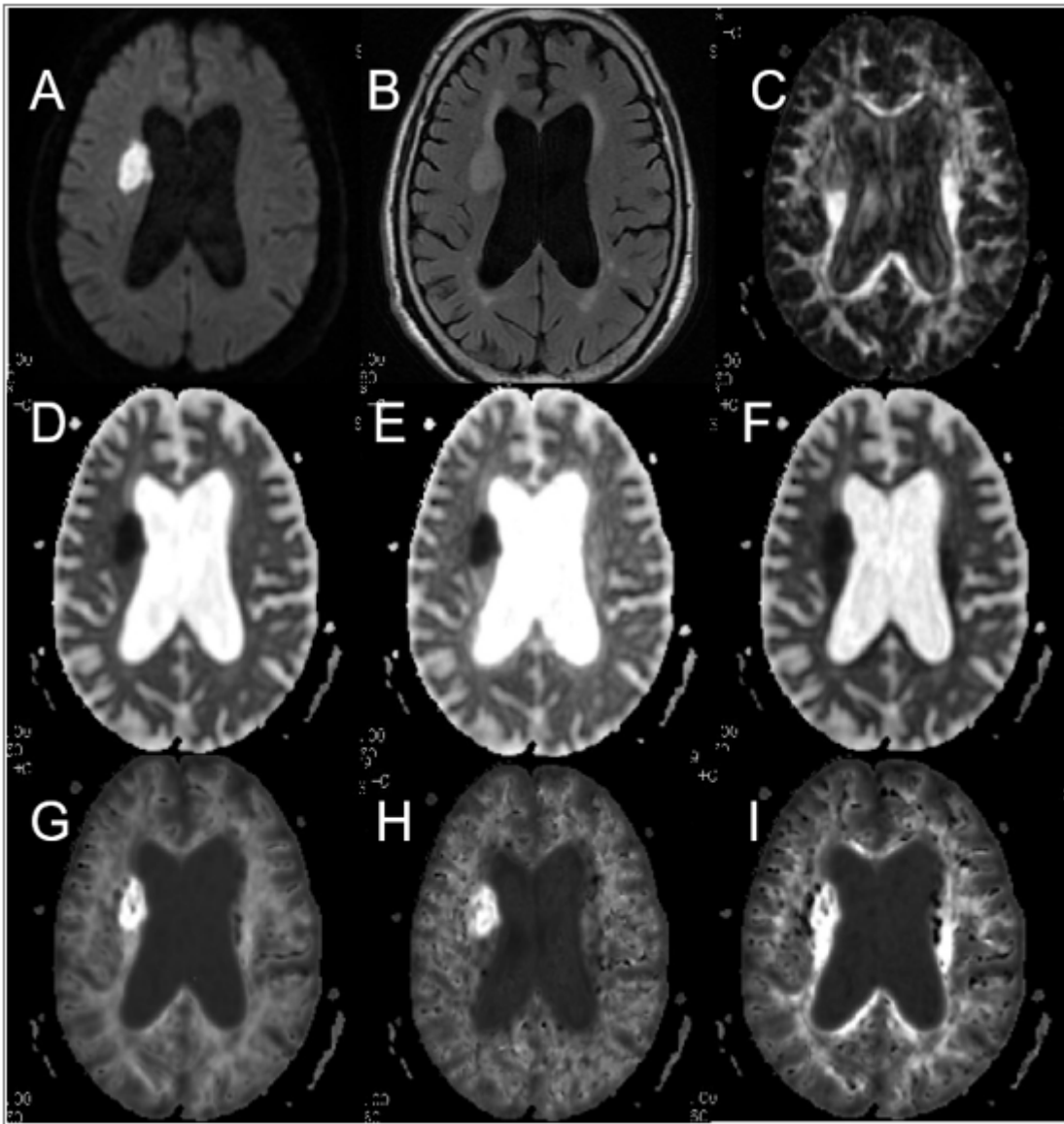


Figure 2

Type I: Parameters of both DKI and DWI were matched; both of them were positive. Parametric maps of DWI and DKI, including FA, MD, Da, Dr, MK, Ka, and Kr, for acute cerebral infarction lesions in the deep white matter besides the right lateral ventricles. A, DWI; B, T2-FLAIR; C, FA; D, MD; E, Da; F, Dr; G, MK; H, Ka; I, Kr DWI, diffusion-weighted magnetic resonance imaging; DKI, diffusion kurtosis imaging; FA, fractional anisotropy; MD, mean diffusivity; Da, axial diffusivity; Dr, radial diffusivity; MK, mean kurtosis; Ka, axial kurtosis; Kr, radial kurtosis; T2-FLAIR, T2-weighted fluid-attenuated inversion recovery

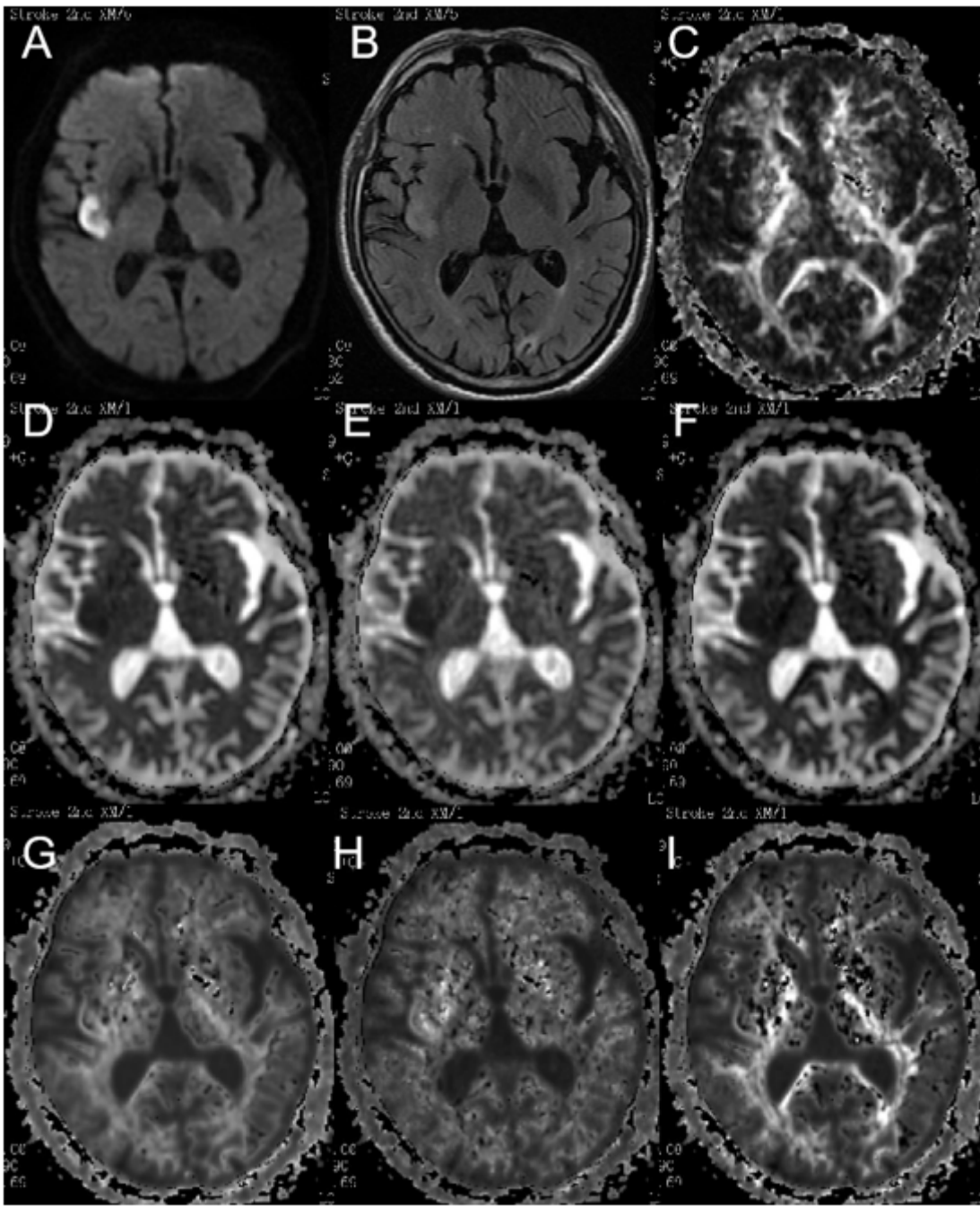


Figure 3

Type II: DKI and DWI parameters were mismatched; DWI parameters were positive, whereas DKI parameters were negative. Parametric maps of DWI and DKI, including FA, MD, Da, Dr, MK, Ka, and Kr, for acute cerebral infarction in the right insular lobe. A, DWI; B, T2-FLAIR; C, FA; D, MD; E, Da; F, Dr; G, MK; H, Ka; I, Kr DWI, diffusion-weighted magnetic resonance imaging; DKI, diffusion kurtosis imaging; FA, fractional anisotropy; MD, mean diffusivity; Da, axial diffusivity; Dr, radial diffusivity; MK, mean kurtosis; Ka, axial kurtosis; Kr, radial kurtosis; T2 FLAIR, T2-weighted fluid-attenuated inversion recovery

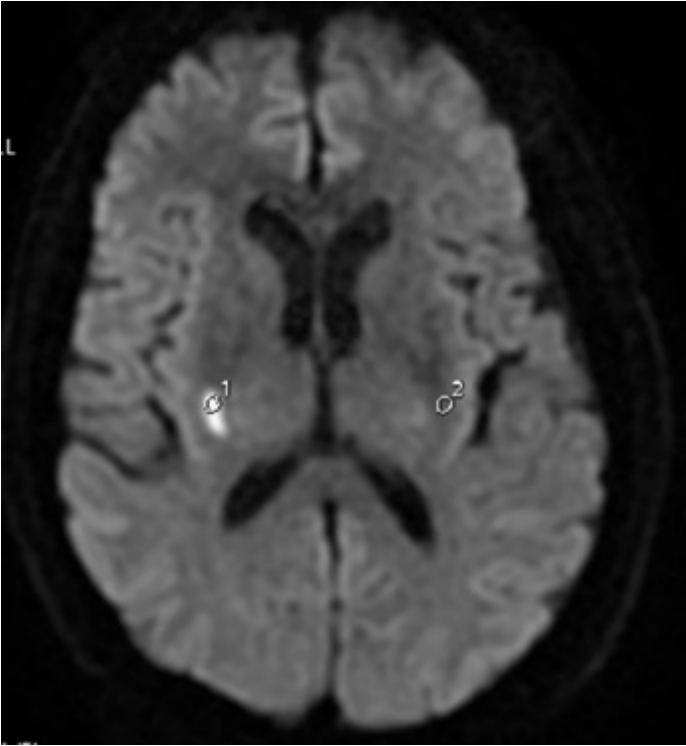


Figure 4

ROIs (maximal areas in the center of the lesions) were outlined within the most severe areas of each lesion according to each independent parametric map. Same-sized ROIs were located in the corresponding normal brain regions of the contralateral hemisphere. ROI, region of interest

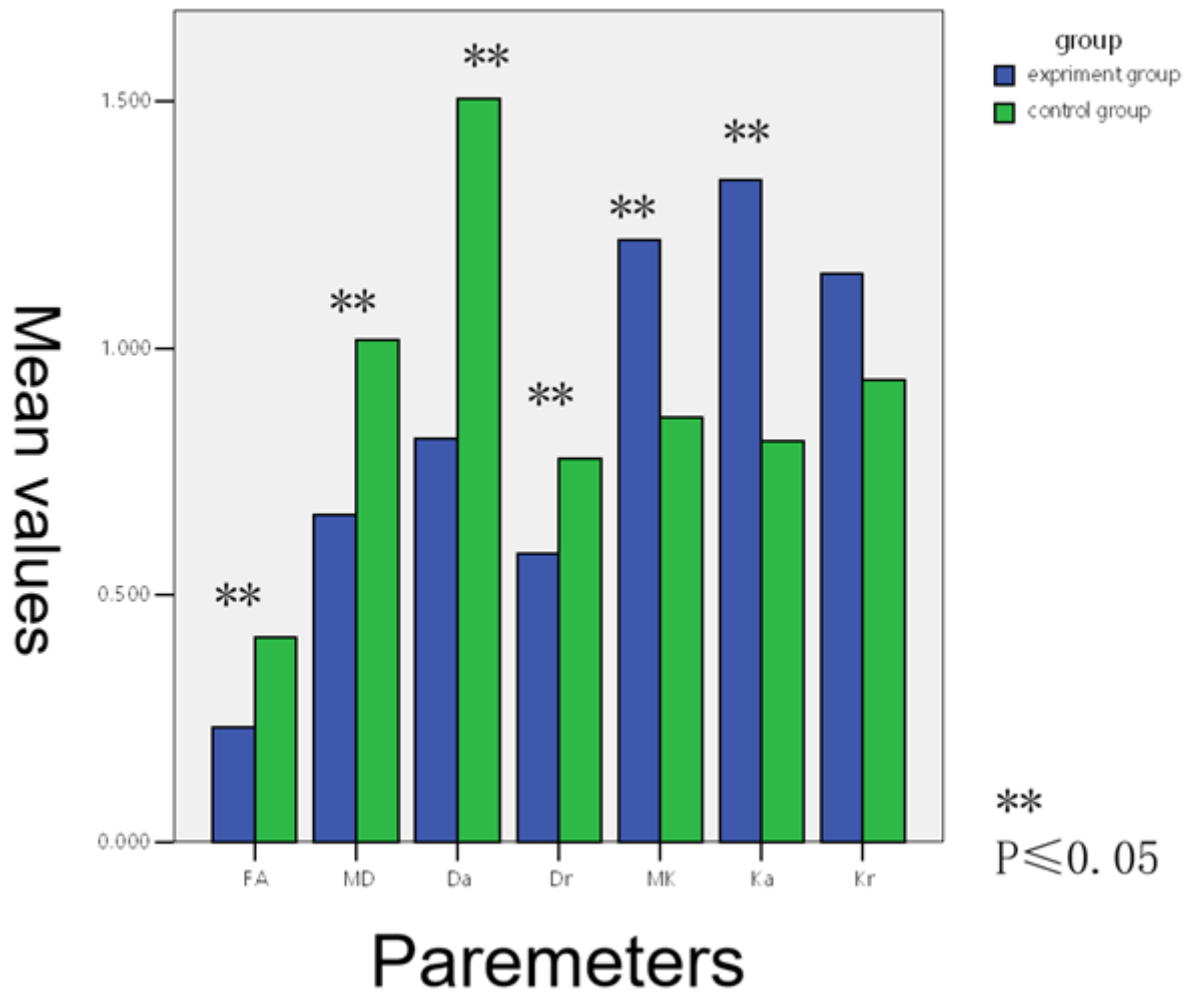


Figure 5

Box plot shows the values of FA, MD, Da, Dr, MK, Ka, and Kr of acute stroke patients with type I stroke lesions. Group 1, experiment group; group 2, control group FA, fractional anisotropy; MD, mean diffusivity; Da, axial diffusivity; Dr, radial diffusivity; MK, mean kurtosis; Ka, axial kurtosis; Kr, radial kurtosis

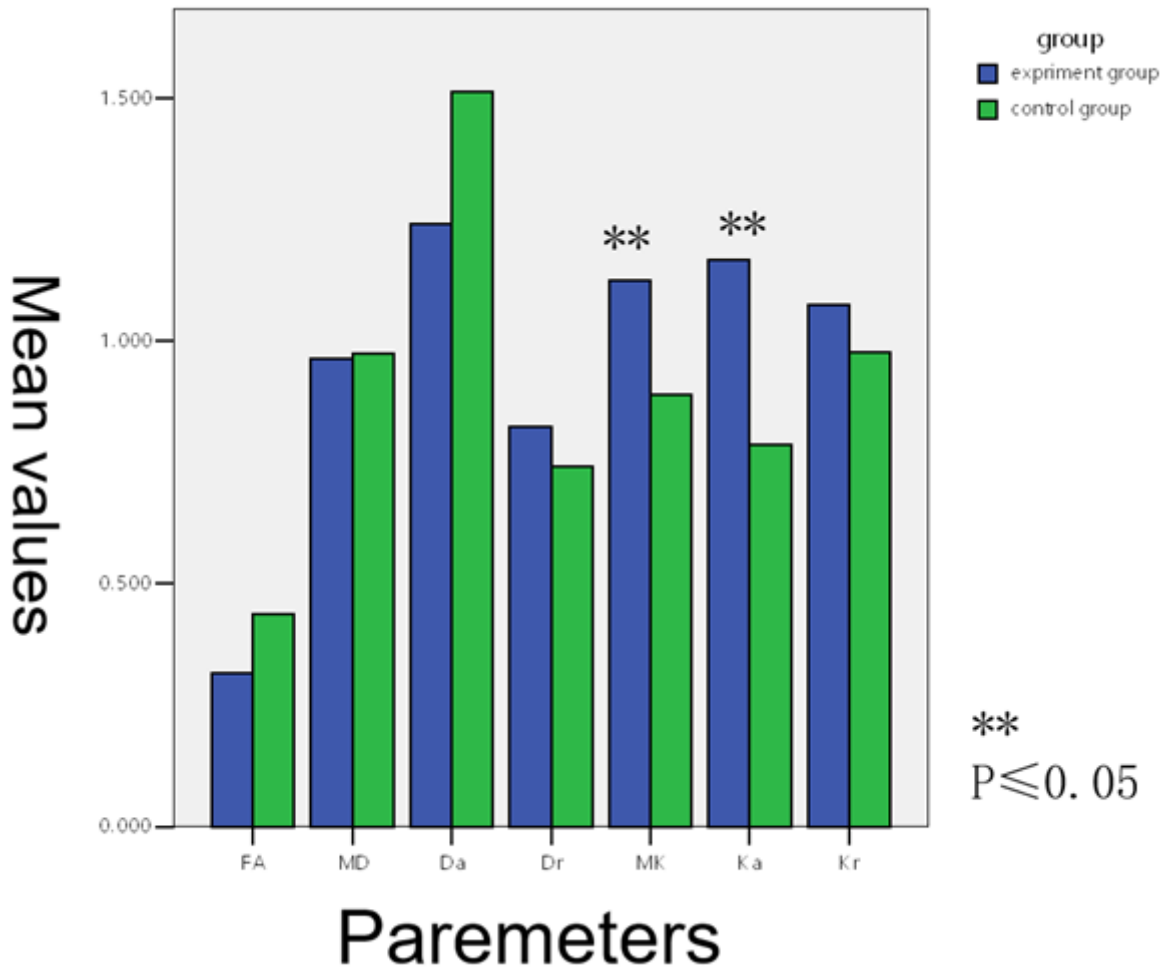


Figure 6

Box plot shows the values of FA, MD, Da, Dr, MK, Ka, and Kr of acute stroke patients with type II lesions. Group 1, experiment group; group 2, control group FA, fractional anisotropy; MD, mean diffusivity; Da, axial diffusivity; Dr, radial diffusivity; MK, mean kurtosis; Ka, axial kurtosis; Kr, radial kurtosis